Measurement Technique for Characterizing Memory Effects in RF Power Amplifiers

Joel H. K. Vuolevi, Timo Rahkonen, *Member, IEEE*, and Jani P. A. Manninen

***Abstract*—Memory effects are defined as changes in the amplitude and phase of distortion components caused by changes in modulation frequency. These are particularly important in cancelling linearizer systems, e.g., when distortion is reduced by similar distortion in the opposite phase. This paper begins by describing electrical and electrothermal causes for memory effects. A three-tone test setup is then constructed to measure the phase of third-order intermodulation distortion products. This paper also presents the measured results for a bipolar junction transistor and a MESFET amplifier.**

***Index Terms*—Electrical memory effects, predistortion, thermal memory effects, thermal power feedback, three-tone test setup.**

I. Introduction

THE adjacent channel power ratio (ACPR) is a commonly used figure-of-merit to describe linearity in modern telecommunication systems. It is defined as the power ratio between a wanted signal and unwanted distortion, measured over the signal band, as presented in Fig. 1(a).

In power amplifier design, the ACPR is often used as a figure-of-merit for linearity [1], [2]. However, designers of power amplifiers need to understand the mechanisms that generate the ACPR. Therefore, a two-tone test signal with varying tone spacings and amplitudes, as presented in Fig. 1(b), has to be employed to find out how distortion responds to changes in amplitude and tone spacing. If the amplifier behaves properly over the tone-difference range of the two-tone signal over a wide range of amplitudes, the amplifier can be expected to also behave correctly with wide-band signals.

Section II of this paper discusses modulation bandwidth limitations (i.e., memory effects) and identifies electrical and electro-thermal causes of memory. Section III introduces a new technique for measuring the memory of an amplifier and discusses the advantages and limitations of the method. Finally, Section IV presents the measured results for a bipolar junction transistor (BJT) and a MESFET amplifier with an analysis of the relationship between node impedances and memory effects.

II. Memory Effects

Amplifiers are traditionally modeled with a memoryless input–output relation, which can be written as

$$y = a_0 + a_1 \cdot x + a_2 \cdot x^2 + a_3 \cdot x^3 \tag{1}$$

Manuscript received December 12, 2000.

The authors are with the Electronics Laboratory, Department of Electrical Engineering, University of Oulu, RIN-90014 Oulu, Finland (e-mail: joel.vuolevi@ee.oulu.fi).

Publisher Item Identifier S 0018-9480(01)06147-6.

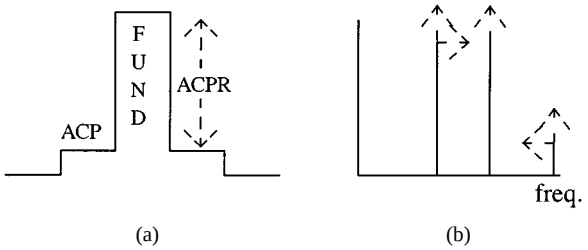

Fig. 1. (a) Spectrum of a modulated signal. (b) Two-tone test with varying tone difference and amplitude.

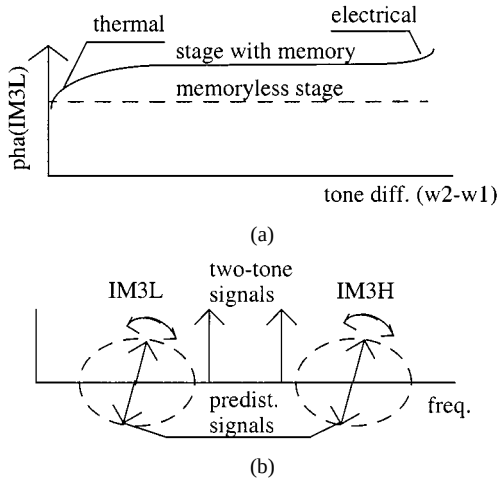

Fig. 2. Definition of memory effect and limited cancellation performance.

where $a_o - a_n$ are complex coefficients. If a two-tone signal

$$x = A \cdot \cos(\omega_1 \cdot t) + A \cdot \cos(\omega_2 \cdot t) \tag{2}$$

is applied, the amplitude for both the lower and upper third-order intermodulation (IM3) sidebands can be written as

$$\text{IM3} = 3/4 \cdot a_3 \cdot A^3. \tag{3}$$

It can be seen from (3) that IM3 sidebands are not functions of tone spacing in (1). Furthermore, the amplitude of IM3 sidebands increases exactly to the third power of the input amplitude. Unfortunately, power amplifiers do not behave like this. Their behavior is explained in more detail in Fig. 2(a), where the phase of the IM3 tone is presented as a function of the tone difference of a two-tone signal.

Equation (3) yields a straight line as a function of tone difference, as shown by the dashes in Fig. 2(a). The solid curve presents the phase of the IM3 component of a real power-amplifier device. Such modulation bandwidth limitations that are amplitude or phase deviations of intermodulation (IM) responses caused by the tone difference of a two-tone signal are called

memory effects. It is important to emphasize that distortion itself is not a memory effect, but any nonconstant distortion behavior at different modulation frequencies (tone spacings) can be regarded as one.

Smooth memory effects are not harmful for the power amplifier itself. A phase rotation of 10°–20° or an amplitude change of less than 0.5 dB has no dramatic effect on the device's ACPR performance. However, the situation changes completely when linearization is used to cancel IM sidebands. Predistortion, for example, is a linearization method that produces signal components that are of equal amplitude and opposite phase compared to the distortion products. This is demonstrated in Fig. 2(b). Since IM3 sidebands rotate back and forth with changes in modulation frequency, but predistortion signals usually have a constant phase, it is evident that memory effects seriously limit the maximum achievable cancellation performance of the method. Unfortunately, the majority of other linearization methods also suffer from the same defect. As a consequence, memory effects render the use of linearization ineffective for a number of applications.

A. Electrical Memory Effects

To determine the causes of memory effects, it is important to investigate why the real power-amplifier device differs from the polynomial model. We shall first turn our attention to electrical causes of memory.

The principle of modeling nonlinear behavior by means of a polynomial is insufficient because it fails to take two additional factors into account. Firstly, although (1) models the input–output relation, the relation in its plain form neglects the fact that distortion components in one node create higher order ones, and so on. For example, the nonlinearity of base–emitter resistance (rpi) in bipolars causes nonlinear responses at the base of the transistor, and these nonlinear responses generate new products either in the rpi or other nonlinearity mechanisms. Secondly, (1) does not hold because there is always more than one nonlinearity mechanism present in the transistor amplifier. Thus, to gain an insight into distortion mechanisms, the transistor amplifier will be considered as a cascade of two polynomials (still highly simplified). The first polynomial can be regarded as a nonlinear transfer function between $v\mathrm{in}$ and $v\mathrm{be}$, and the second between $v\mathrm{be}$ and $i\mathrm{out}$.

Fig. 3(a) presents the output of the first block [or (1)], and the amplitude of the IM3 component can be calculated from (3). This multitone signal is the input signal for the second block, and the output IM3 now combines with other frequency components. For example, the envelope signal ($w2$–$w1$) and the upper two-tone signal ($w2$) will be mixed with the second-order nonlinearity of the latter block, which results in the generation of an IM3 signal. Similarly, the second harmonic of the upper input signal ($2w2$) and the lower input signal from the negative frequency side ($-w1$) will produce an IM3 signal. As a result, IM3 sidebands are affected not only by fundamental voltage waveforms, but also by the voltage waveforms of the different nodes at the frequency of the envelope ($w2$–$w1$). In addition, the second harmonics ($2w1$ and $2w2$) also affect the IM3 sidebands. The question is how to control the voltage waveforms of the different nodes and frequency components. Since the nonlinearities of the circuit components can be considered as current sources, their voltage waveforms can be affected by node impedances [4]. The composition of IM3 in the real power amplifier device is sketched in Fig. 3(b) with nonlinearities up to the third order. The greatest part of the distortion is produced by third-order distortion mechanisms, which are affected by fundamental impedance. However, second-order mechanisms generated by the envelope and second harmonic frequencies (and impedances) also have a significant effect on IM3 distortion.

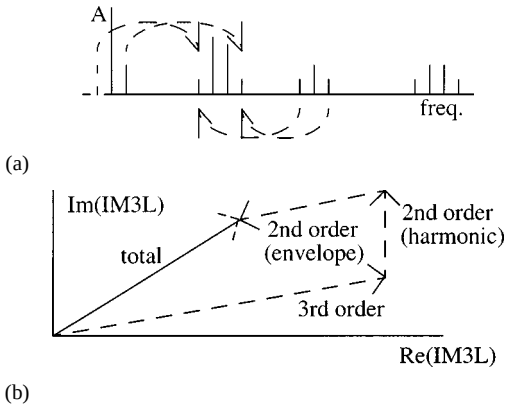

Fig. 3. (a) Spectral components produced by nonlinearities up to the third order. (b) Composition of IM3.

Node impedances consist of two parts: internal impedance of the transistor and external impedance. External impedance also comprises two parts: the impedance of the matching network and that of the bias network. The combined effects of these impedances must be considered in the design of well-behaving node impedances.

Electrical memory effects are caused by varying envelope, fundamental or second harmonic impedances at different modulation frequencies. Of these, fundamental impedance can easily be kept constant over the entire modulation frequency range because it deviates maximally 1% from the center frequency in most RF systems. The range of the second harmonic impedance is also quite narrow, and matching is simple if harmonic traps for attenuating harmonic responses are avoided. Such traps cause huge impedance variations and are a significant source of memory. As fundamental and second harmonic impedances play a minor role, the major part of the memory is produced by envelope impedances. Envelope frequency varies from dc to the maximum modulation frequency, which can be as high as a few megahertz. The output impedance, for example, must be constant or very low over this region in order to avoid memory effects. Since node impedance consists of bias impedance, and a large time constant is needed in bias networks as an energy storage, memory effects are unavoidable. However, with careful design, electrical memory effects can be limited to those caused by bias networks. A thorough analysis of distortion mechanisms lies beyond the scope of this paper, but the distortion mechanisms and memory effects of the BJT are analyzed in detail in [3] and [4].

B. Thermal Memory Effects

Thermal memory effects are caused by electro-thermal couplings, and these affect low modulation frequencies up to a few

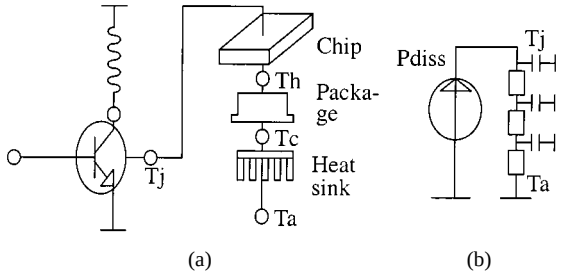

Fig. 4. Heat flow from the device. (a) Physical and (b) electrical lumped-element models.

megahertz. The dissipated power of the BJT, for example, can be expressed as

$$p_{\mathrm{DISS}} = v_c \cdot i_c \tag{4}$$

where v_c is the collector voltage and i_c is the collector–emitter current. Since two first-order (fundamental) signals are multiplied together, the spectrum of the dissipated power always includes second-order signal components (envelope and second harmonics). Temperature variations caused by the dissipated power are determined by thermal impedance, which describes the heat flow from the device. Due to the finite mass of the component, thermal impedance in the active device is not purely resistive, but instead, it forms a distributed low-pass filter with a wide range of time constants. This means that the temperature changes caused by the dissipated power do not occur instantaneously; rather, frequency-dependent phase shifts always exist. Moreover, the surface of silicon reacts surprisingly quickly, and temperature fluctuations of several degrees can be seen over a bandwidth from 100 K to 1 M. More detailed analyses can be found in [5]–[8], and it is suffice to say here that the magnitude of Zth is significant up to hundreds of kilohertz, and that not only the silicon chip, but also the layers of the package and heat sink, have to be considered, as shown in Fig. 4.

Since only the dc and envelope components of the dissipated power fit into the passband of the thermal filter, the temperature of the chip gets the following simple form:

$$T = T_{\mathrm{AMB}} + R_{\mathrm{TH}} \cdot p_{\mathrm{DISS}}(\mathrm{dc}) + Z_{\mathrm{TH}}(\omega_1 - \omega_2) \cdot p_{\mathrm{DISS}}(\omega_1 - \omega_2). \tag{5}$$

The temperature of the chip consist of three components: first, the temperature is directly proportional to the ambient temperature. The other two components are the thermal resistance multiplied by the dc power dissipation, and the envelope component multiplied by the thermal impedance at that frequency. It is interesting to note that the third term in (5) includes frequency, which means that the temperature at the top of the chip changes dynamically with the signal applied. If any of the electrical parameters of the transistor are affected by temperature, thermal memory effects are unavoidable. This mechanism in which dynamic self-heating causes electrical distortion is known as thermal power feedback (TPF).

A block diagram of TPF is shown in Fig. 5, and the basic amplifier is considered as a memoryless polynomial stage. Thermal impedance describes the relationship between dissipated power and temperature and block K describes the relationship between

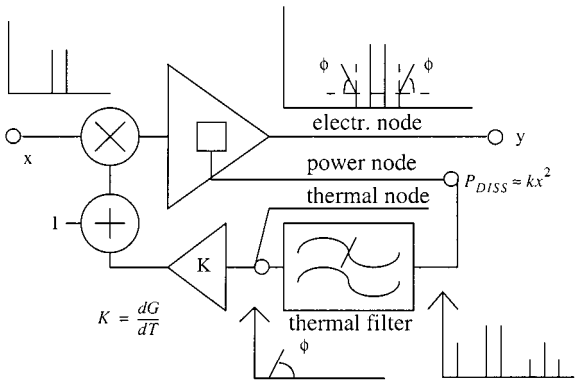

Fig. 5. Block diagram of TPF.

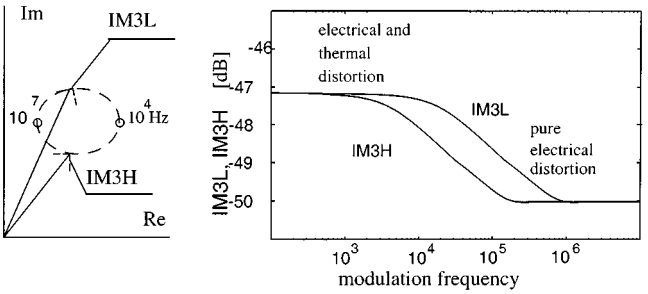

Fig. 6. Representation of: (a) IM3 caused by distortion of the basic amplifier and TPF and (b) linearity deterioration caused by TPF at low modulation frequencies.

temperature and the gain of the amplifier. In this paper, only the gain of the amplifier is considered to be temperature dependent. In practice, however, output conductance and capacitances, for example, are also temperature dependent. Some of the circuit parameters of the transistor are always a function of temperature, and since temperature-compensated external bias networks are insensitive to junction temperature, they are far too slow to compensate for its effects. Thus, no improvement can be expected in terms of TPF.

A two-tone input signal is modulated by gain variations at the envelope frequency, thereby generating IM3 sidebands. Since the phase response of the thermal filter at the positive envelope (causing higher third-order intermodulation (IM3H) product) is opposite to that at the negative envelope (lower third-order intermodulation (IM3L) product), the IM3 sidebands are produced by TPF spin in opposite directions as a function of modulation frequency, as shown in Fig. 6. A linearity decrease of several decibels is observed at low modulation frequencies, and the symmetry between the sidebands is lost at some modulation frequencies. Due to that, problems caused by TPF are considerably more serious in connection with predistorters. For a more detailed analysis of TPF, see [6] and [8].

III. Measuring Memory Effects

Memory effects are rather difficult to measure. Spectrum analyzers may be used to measure sideband amplitudes, but they do not provide phase information. Although a system comprising two network analyzers is capable of yielding phase information about the fundamental signals in a two-tone test, as explained

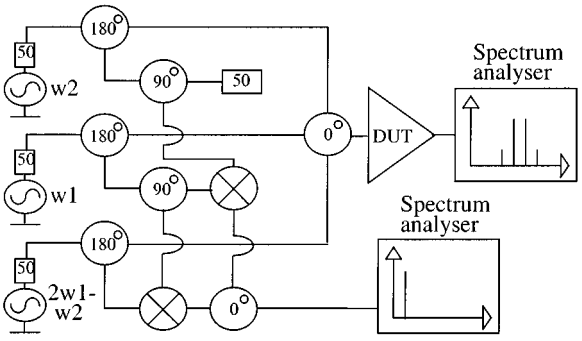

Fig. 7. System for measuring memory effects.

in [9], these measurements only produce information about the memory effects of the fundamental signal. As explained in Section II, this procedure does not provide complete information about the memory effects of the IM components, which is a point of primary interest in terms of linearization.

Some systems for measuring the phase of the harmonics have been developed [10] and at least one for the IM3 relative phase [11]. These are based on a diode that is used as a reference nonlinearity, producing a constant-phase IM3 component over a modulation band. In [11], a two-tone signal is applied to the device-under-test (DUT) and reference nonlinearity, and the output signals are added together. This sum consisting of the constant-phase reference IM3 and measured IM3 is tried to cancel by tuning manual attenuators and phase shifters in order to find the phase of the IM3 component at the output. The drawback of the method is that only a relative phase information with respect to amplitude can be obtained and the validity of this information is dependent on the reference nonlinearity that must be an ideal third-order distorter to avoid the errors. Further, no tone-difference sweep was reported in [11].

A. Test Setup and Calibration

The measurement system introduced in Fig. 7 can be employed for measuring both the amplitude and phase responses of IM signals in order to characterize the memory effects of the amplifier. The key idea behind the measurements is that an IM distortion signal is applied together with a two-tone signal to the input. By adjusting the amplitude and phase of the test signal, the output IM3 can be cancelled. Furthermore, memory effects can be measured by sweeping the tone difference of the two-tone signal over a range of modulation frequencies. The test setup presented here does not actually measure the IM3 component at the output, but it instead measures the optimum input signal that creates maximum cancellation to the output. That is a highly significant advantage because it allows the measurement results to be used directly as required characteristics for predistortion circuits.

The calibration of the measurements is somewhat complicated. The basic idea is that two downconverted signals are compared to detect the phase of the IM3 signal. A two-tone input signal is mixed down to the envelope frequency, along with the lower signal of the two-tone signal and the IM3L signal. These two are brought to a resistive power combiner, and by adjusting the amplitude and phase of the IM3L signal, the signal at the output of the power combiner vanishes. The phase shift of these two equally spaced frequency components is fixed and depends only on the phase shift of the cables and power splitters, which can be easily measured and calibrated. After that, the amplitude and phase of the IM3L signal is adjusted again, until the IM3L component at the output of the amplifier disappears. In this way, the phase difference between these two situations in which the signal component vanishes gives the phase of the IM3L component of the amplifier (although the calibration of the cables has to be considered). On the other hand, the amplitude of the IM3L generated by the stage is much easier to obtain because the attenuation of the cables and power splitters/combiners is easy to take into account. The IM3H of the stage can also be measured similarly, either simultaneously or separately. The fourth signal generator for the IM3H can by applied for the simultaneous measuring of both the lower and upper IM3 sidebands. After all, the sidebands can be measured independently by changing the frequency of the IM3L signal generator to the frequency of the IM3H and by changing the frequencies of the lower and upper two-tone signals.

B. Accuracy and Automation

A test setup was constructed for the LabView environment to automatize the measurements. The setup was designed to be fully automatic with no need for manually tunable attenuators or phase shifters. All tuning for the IM3 sidebands and fundamental signals was performed by means of three RF signal generators. In addition, two spectrum analyzers were used to measure the amplitudes of the IM3 sidebands and envelope. All measurement equipment was controlled via an HP general-purpose interface bus (GPIB) cable. Each measurement took about 15 min, and a complete series of measurements over a range of modulation frequencies lasted a few hours. The optimization of search algorithms will reduce the duration of each individual measurement to less than 5 min.

The accuracy of the measurements is an important consideration. There are two different kinds of measurement errors: those that cannot be calibrated (systematic errors) and those that can be taken into account by careful calibration. Systematic errors are dominated by the cancelled IM3 amplitude. For example, if an IM3 level of -40 dBc is detected at the output of the stage, and it can be cancelled to -70 dBc, this 30-dB cancellation performance requires amplitude or phase error to be less than 0.25 dB or 1° [12]. The cancelled IM3 level is usually limited by the noise floor of the spectrum analyzer or phase noise of the signal generator. As a result, high-performance measurement equipment have to be used to significantly reduce the errors. Unfortunately, errors of more than 1° were observed, and calibration was required to improve the performance of the test setup. It was found that the phase of some inexpensive RF signal generators is a slight function of the amplitude, and that more serious phase jumps occur at fixed amplitude steps when switching the attenuators to the RF path inside the signal generator. Nevertheless, these phase errors can be calibrated, and by using a high-performance RF signal generator, their role can be diminished. Furthermore, some signal generators suffer from a very low-frequency phase drift. The effects of this defect can be avoided by rechecking the cancelling phases

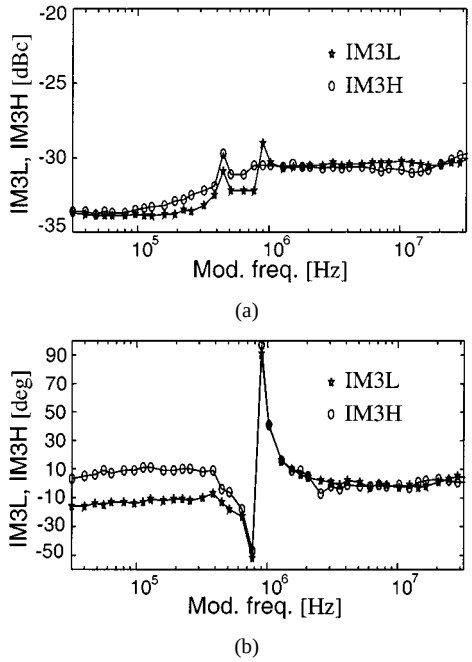

Fig. 8. Measured: (a) amplitude and (b) phase of optimum predistortion signals for the Philips BFG 11 common-emitter amplifier.

at the end of each measurement. Also, any test setup will exhibit a degree of unwanted IM so that, even if a signal generator is not applied at IM3, signal components can still be observed there. When measuring very linear stages, this may turn out to be a real problem, but, fortunately, the test setup itself could be calibrated by measuring it without the DUT. The level of unwanted IM responses was found to be −70 dBc, but the use of high-quality mixers, power combiners, power splitters, and cables can easily reduce the figure by more than 10 dB.

IV. Measured Results

A. Memory Effects in a BJT Stage

A Philips BFG 11 amplifier designed according to the data sheet [13] provided by the manufacturer was measured at the supply and bias voltages of 3 V and 740 mV, respectively. The tone spacing of the fundamental tones was swept from 32 kHz to 32 MHz around the center frequency of 1.8 GHz.

The amplitude (in decibels relative to carrier at the input compared to the input signal) and phase of the IM3 components are given in Fig. 8. As expected, the amplitude of the required cancelling signal at the input is directly proportional to the IM3 level at the output. However, the phase of the IM3 is interesting: at high modulation frequencies (above 500 kHz), the phases of both sidebands were equal, but at low modulation frequencies, the phases started to deviate such that a 20° phase offset was detected at 32 kHz. Since no electrical time constant of that size existed in the circuit, it is evident that these low-frequency memory effects were caused by TPF.

A phase jump was also observed at 1 MHz in the modulation response. A schematic of the amplifier is presented in Fig. 9(a), and the collector impedance at the envelope frequency is given in Fig. 9(b). It was verified by varying the *LC* product in the bias network that it actually is the baseband *LC* resonance that

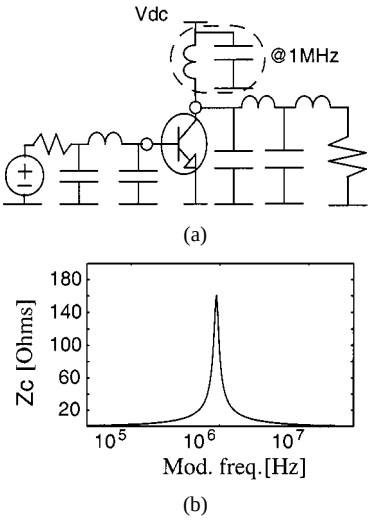

Fig. 9. (a) Schematic of the BJT amplifier. (b) Measured impedance of the collector node as a function modulation frequency.

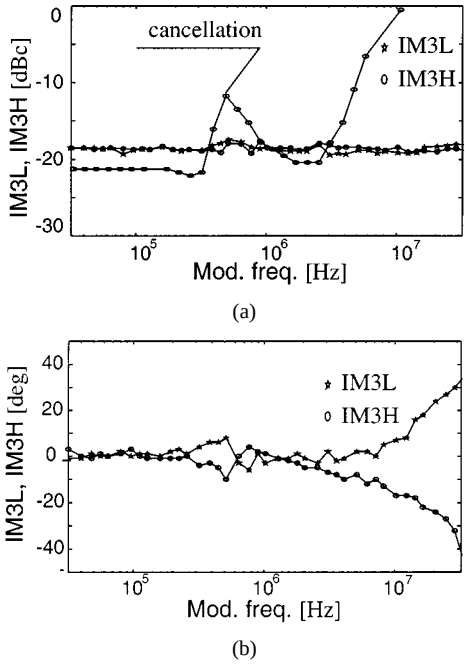

Fig. 10. Measured: (a) amplitude and (b) phase of the optimum predistortion signals for the Infineon CLY2 common-source amplifier. [(a) also shows the achieved cancellation with memoryless RF predistortion.]

causes the large phase jump in the IM3 phase. It is interesting to note that this phase jump was not detected in simulations using the SPICE BJT model due to inadequate output conductance modeling.

B. Memory Effects in a MESFET Stage

During this part of the research, an Infineon CLY2 amplifier [14] was designed and measured. Its drain bias voltage and current were set to 3 V and 20 mA, respectively, and the tone spacing of the fundamental tones was swept from 32 kHz to 20 MHz at the center frequency of 1.8 GHz.

The amplitude (in decibels relative to carrier at the input) and phase of the IM3 components are given in Fig. 10. The amplitude of the required cancelling signal remains nearly constant

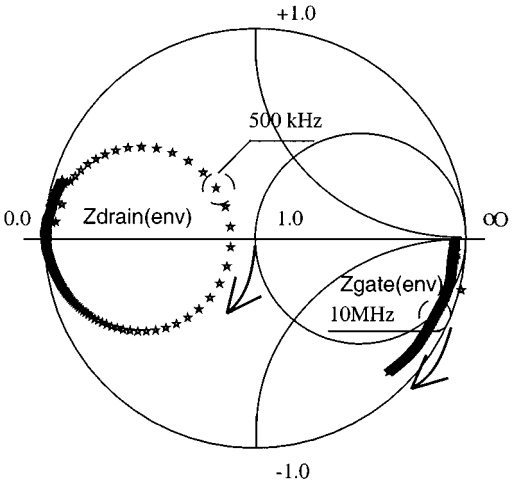

Fig. 11. Measured gate and drain node impedance of the CLY 2 amplifier from 32 kHz to 32 MHz. $Znom = 50\,\Omega$.

over the entire modulation band. This does not mean, however, that memory effects did not occur. The phase of the IM3 started to deviate above 1 MHz, and a phase difference of 40° was found to exist at 30 MHz. In addition, a smooth phase deviation of 10° around 500 kHz was also detected, as seen in Fig. 10. Thermal memory effects were not detected at low modulation frequencies because the MESFET was biased to be quite nonlinear, resulting in a predominance of purely electrical causes of distortion.

Section II indicated that the majority of electrical memory effects are caused by impedances at the envelope frequency and, therefore, the gate and drain node impedances of the amplifier at that frequency are presented in Fig. 11. The device's drain impedance is fairly constant over the modulation band, but the value produced at 500 kHz is relatively high. This has an impact of 10° on the phase of the IM3 response, caused by the *LC* time constant in the drain bias circuit. Resistive gate biasing was used to avoid memory effects at the input, but at high modulation frequencies, gate impedance starts to decrease due to the Cgs. As a result, the modulation response starts to spin. The measurements were confirmed using a memoryless third-order RF predistorter [15] and looking at the cancellation of IM3 as a function of modulation frequency presented in Fig. 10(a). Decreased cancellation performance indicates amplitude and/or phase deviations in IM3 components, and very good correlation with the measured memory and decreased cancellation performance is detected. In conclusion, impedances at the envelope have to be designed carefully to ensure flat modulation responses and good cancellation performance.

V. Summary

Memory effects are a significant source of difficulties in RF power stages. If the amplitude or phase of the distortion component is a function of the modulation frequency, the stage exhibits memory. Memory effects are harmful for most linearizers, such as predistorters, by imposing serious limitations on their cancellation performance.

Memory effects can be divided into two classes: electrical and electro-thermal effects. Thermal memory effects affect low modulation frequencies up to a few megahertz, while purely electrical memory effects are usually caused by the source and/or load impedances at the envelope frequency. Some of the nonlinearity mechanisms generating memory effects are quite complicated and, due to inadequate device modeling, commercial circuit simulators cannot always be used to characterize them.

Memory effects can be characterized by measurements, which provides information about the expected cancellation performance, while also revealing from which frequencies the effects are generated. The test setup presented in this paper is capable of providing not only amplitude, but also phase information of the distortion sidebands. The measurements demonstrated the effects of the low-frequency source and load impedance on the modulation response. The measurements also showed good agreement between memory effects and cancellation performance of a memoryless predistorter. It can be concluded that impedances have to be considered very carefully when designing easily linearizable power amplifiers. The measurement technique presented in this paper is capable of providing information that can be used to optimize design and, more importantly, to characterize the requirements for a predistortion device.

References

[1] S. C. Cripps, *RF Power Amplifiers for Wireless Communications*. Norwood, MA: Artech House, 1999.
[2] J. F. Sevic and J. Staudinger, "Simulation of power amplifier adjacent-channel power ratio for digital wireless communication systems," in *IEEE Veh. Technol. Conf.*, vol. 2, 1997, pp. 681–685.
[3] J. Vuolevi and T. Rahkonen, "Intermodulation distortion in common-emitter BJT and HBT amplifiers—Part I: The volterra model," *IEEE Trans. Circuit Syst. II*, to be published.
[4] P. Wambacq and W. Sansen, *Distortion Analysis of Analog Integrated Circuits*. Norwell, MA: Kluwer, 1998.
[5] P. Perugupalli, Y. Xu, and K. Shenai, "Measurement of thermal and packaging limitations in LDMOSFET's for RFIC application," in *Proc. IEEE Instrum. Meas. Technol. Conf.*, vol. 1, 1998, pp. 160–164.
[6] A. R. Hefner and D. L. Blackburn, "Simulating the dynamic electrothermal behavior of power electronics circuits and systems," *IEEE Trans. Power Electron.*, vol. 8, pp. 376–385, Oct. 1993.
[7] A. R. Hefner, "A dynamic electro-thermal model for the IGBT," *IEEE Trans. Ind. Applicat.*, vol. 30, pp. 394–405, Mar./Apr. 1994.
[8] J. Vuolevi and T. Rahkonen, "Third-order intermodulation distortion caused by thermal power feedback," in *Proc. Norchip'99*, Oslo, Norway, pp. 121–125.
[9] W. Bösch and G. Gatti, "Measurement and simulation of memory effects in predistortion linearizers," *IEEE Trans. Microwave Theory Tech.*, vol. 37, pp. 1885–1890, Dec. 1989.
[10] U. Lott, "Measurement of magnitude and phase of harmonics generated in nonlinear microwave two-ports," *IEEE Trans. Microwave Theory Tech.*, vol. 37, pp. 1506–1511, Oct. 1989.
[11] N. Suematsu, T. Shigematsu, Y. Iyama, and O. Ishida, "Transfer characteristic of IM_3 relative phase for a GaAs FET amplifier," in *IEEE MTT-S Int. Microwave Symp. Dig.*, vol. 2, 1997, pp. 901–904.
[12] T. Rahkonen and J. Vuolevi, "Memory effects in analog predistorting linearizing systems," in *Proc. Norchip'99*, Oslo, Norway, pp. 114–119.
[13] "BGF 11/X NPN 2 GHz RF power transistor," Philips Semiconduct., 1995.
[14] "CLY 2 GaAs power MESFET," Infineon Technol., 1996.
[15] J. Vuolevi, J. Manninen, and T. Rahkonen, "Cancelling the memory effects in RF power amplifiers," in *ISCAS 2001*, vol. 1, Sydney, Australia, pp. 57–60.

Joel H. K. Vuolevi was born in Oulu, Finland, in 1975. He received the M.Sc. degree in electrical engineering from the University of Oulu, Oulu, Finland, in 1998, and is currently working toward the Ph.D. degree in electronics at the University of Oulu.

From 1997 to 1998, he was an RF Design Engineer with Nokia Mobile Phones. In 1998, he joined the Electronics Laboratory, University of Oulu. His technical interests concern the field of predistortion techniques and distortion analysis of RF power amplifiers.

Timo Rahkonen (S'88–M'90) was born in Jyvaskyla, Finland, in 1962. He received the Diploma Engineer, Licentiate, and Doctor of Technology degrees from the University of Oulu, Oulu, Finland, in 1986, 1991, and 1994, respectively.

He is currently a Professor in circuit theory and circuit design at the University of Oulu. His research concerns linearization and error-correction techniques for RF power amplifiers and A/D and D/A converters.

Jani P. A. Manninen was born in Rauma, Finland, in 1976. He is currently working toward the M.Sc. degree in electrical engineering at the University of Oulu, Oulu, Finland.

In December 1999, he joined the Electronics Laboratory, University of Oulu. His technical interests include predistortion techniques, RF power amplifier design, and measurement techniques.